LCO CALCULATIONS COMPARED WITH WIND TUNNEL EXPERIMENT FOR 2D FLUTTER MODEL

Wojciech POTKAŃSKI, Zbigniew LORENC, Daniel SZELĄG
Institute of Aviation

Summary

The flutter analysis of modern aircraft search for the lowest (critical) flutter speed under given conditions and the variation of the critical flutter speed with certain system parameters, however static tests and ground vibration tests performed on prototypes show existence of structural nonlinearities that result in LCO. The harmonic linearization and the continuation method, described in the paper, have been successfully used previously to LCO prediction for a two degree of freedom profile with nonlinear pitch stiffness, and a sailplane with nonlinear controls of flaps, ailerons and elevator [10, 18, 22]. The „stiff wing" flutter model, supported by the mechanical system that allows for independent movement and simulation of nonlinear stiffness in „plunge" and „pitch", has been used in wind tunnel LCO tests. The nonlinearities in experiment generated electromechanically have given a possibility to perform effective investigation of the influence of different nonlinear characteristics on LCO. The tests have been performed at the Low Turbulence Wind Tunnel in the Institute of Aviation in Warsaw [15, 23]. Comparison of LCO calculation with continuation approach against wind tunnel results for 2D flutter model with nonlinear stiffness in „plunge" and „pitch" are presented in the paper.

NOTATION

$\{q\}$	– coordinates vector (column matrix),
$[M]$	– mass matrix,
$[K] = [C] + \mathrm{i}[G]$	– complex stiffness matrix,
$[C]$	– stiffness matrix,
$[G]$	– structural damping matrix
$[A(k)]$	– aerodynamics matrix (complex),
$k = \omega \cdot b/V$	– reduced frequency,
ω	– circular frequency,
b	– reference length,
V	– free-stream velocity,
ρ	– free-stream density,
λ	– eigenvalue,
V_F	– flutter speed,
$Re(..)$	– real part of a complex value,
$Im(..)$	– imaginary part of a complex value,
E	– vibration amplitude level,
$M(\beta)$	– hinge moment,
β	– control surface deflection,
E_d	– energy dissipated in one period of oscillation,
a	– location of the rotation axis,
K_{h0}	– (linear) plunge stiffness,
$K_{\alpha 0}$	– (linear) pitch stiffness,
β_h, β_α	– nonlinearity factors,
g_h, g_α	– artificial damping,
M	– mass,
S	– mass static moment relative to the wing rotation axis,
I	– mass moment of inertia relative to the wing rotation axis.

1. INTRODUCTION

In the design of modern aircraft many computer hours are consumed on calculations of aeroelastic problems. The most important of them are flutter analysis. The flutter analysis is therefore concerned to a search for the lowest (critical) flutter speed under given conditions, and the variation of the critical flutter speed with certain system parameters. Static tests and ground vibration tests carried out on prototypes confirm existence of both distributed and concentrated structural nonlinearities. The effect of distributed nonlinearities on the vibration mode shapes can mostly be regarded as negligible. Concentrated nonlinearities occur locally in control mechanisms or in connections between aircraft parts. Nonlinearities of this type are indicated in static tests on the *force-deflection* diagrams or in ground vibration tests on the *frequency-amplitude* diagrams [1, 2]. That effects in additional complications in analysis, because flutter of a non linear system may be of the limited amplitude but on the other hand a non linear system that is stable with respect to small disturbances may be unstable with respect to large ones. The nonlinearities in flutter calculations can be handled either by direct integration of equations of motion in the time-domain or by iterative search in frequency-domain [2, 4]. In both methods finite amplitude limit-cycle solution are the targets. For systems with concentrated structural nonlinearities the harmonic linearization [5] method is applied and equivalent stiffness and damping are obtained for a given constant-amplitude harmonic motion. Earlier works [2, 4] confirm the efficiency of iterative process for systems having two nonlinearities. The iteration method is based on the assumption that the aircraft motion is harmonic. Consequently, all nonlinearities of the structure must be *harmonically equivalent* [10] because the classical, linear method is used in each iteration step. One of recent developments in numerical analysis is a class of *continuation methods* [11]. Continuation method can be successfully applied to flutter calculation of systems without structural nonlinearities [12]. Application of a continuation method to the flutter analysis for systems with interacting structural nonlinearities is presented on examples of two degrees of freedom profile with non-linear plunge and pitch stiffness. LCO calculations are compared with wind tunnel experiment for 2D flutter model.

2. FLUTTER EQUATIONS

The methods well known in practical flutter analysis are based on the solution of flutter equation in the frequency domain. The fundamental assumption is that the motion of an aircraft is time-harmonic, which is strictly satisfying only on a boundary between stable and unstable motion. The neutrally stable aircraft motion is described by the flutter equation

$$\left(-\omega^2\left[M\right]+\left[K\right]\right)\{q\}=\rho\omega^2\left[A(k)\right]\{q\}, \tag{1}$$

where: {q} – coordinates vector (column matrix),
[M] – mass matrix,
[K] – stiffness matrix (complex),
[A(k)] – aerodynamics matrix (complex),

which elements are functions of the reduced frequency:

ω – circular frequency,
b – reference length,
V – free-stream velocity,
ρ – free-stream density.

The complex stiffness matrix:
[K] = [C] + i[G] is a sum of a stiffness matrix [C] and a structural damping matrix [G].

The flutter equation (1) (for an assumed value of reduced frequency k) is a system of homogeneous linear equations with the parameter.

$$\left(\omega^2\left([M]+\rho\left[A(k)\right]\right)-[K]\right)\{q\}=0. \tag{2}$$

Non trivial (complex) solution vector can be obtained with accuracy to constant multiplier and should be normalized (for example to unit length and assumed phase)

$$\left\{q^H\right\}\{q\}=1, \tag{3}$$

$$\mathrm{Im}\left(q_n\right)=0, \tag{4}$$

where: Im (q_n) – imaginary part of n-th element of $\{q\}$ and $\{q^H\}$ – hermitian transpose of $\{q\}$.

The assumed value k and the (real) parameter ω, for which a solution of (2) exist, must satisfy the equation

$$k=\frac{\omega\cdot b}{V}. \tag{5}$$

When a proper combination of $k-\omega$ is found, then the flutter problem is solved and the flutter speed V, flutter frequency ω and the flutter mode $\{q\}$ are evaluated.

3. CLASSICAL SOLUTION

The classical way to find a solution of the flutter equation is the transformation of (2) to an eigenvalue problem

$$\left[D(k)\right]\{q\}=\lambda\{q\}, \tag{6}$$

where

$$\left[D(k)\right]=\left([M]+\rho\left[A(k)\right]\right)^{-1}[K] \tag{7}$$

and

$$\lambda=\frac{\omega^2}{1+ig}, \tag{8}$$

where g is the artificial damping which must be (in calculation) added to, or subtracted from the dynamic system (an aircraft) to preserve the harmonic motion ($V-g$ method).

From (8) result

$$\omega=\frac{|\lambda|}{\sqrt{\mathrm{Re}\,\lambda}};\qquad g=\frac{\mathrm{Im}\,\lambda}{\mathrm{Re}\,\lambda};\qquad \text{and}\qquad V=\frac{\omega\cdot b}{k}; \tag{9}$$

The eigenproblem (6) is solved for a set of reduced frequencies k and (9) are interpreted (graphically) on $V-g$ and $V-\omega$ diagrams. Critical conditions (neutrally stable motion) correspond to $g=0$. The lowest value V for $g=0$ is the critical flutter speed V_F.

4. CONTINUATION METHOD

Continuation methods are predictor corrector techniques for the solution of systems of non linear equations which are functions of several parameters, defined over a specified range. Typically there is one more unknown than equations. One of unknowns is chosen as the continuation parameter, and is fixed during the corrector phase in order to give the same number of equations as unknowns. For calculation economy it is important to pick the largest possible predictor step while maintaining convergence in the corrector phase.

The flutter equation (2) ($V-g$ version) with the normalization equations (3, 4) completed by (5), form the set of $2n+3$ real equations

$$\left(\omega^2\left(\left[M\right]+\rho\left[A(k)\right]\right)-(1+ig)\left[K\right]\right)\{q\}=0, \tag{10}$$

$$\left\{q^H\right\}\{q\}-1=0,$$

$$\mathrm{Im}\left(q_n\right)=0,$$

$$V-\frac{\omega\cdot b}{k}=0,$$

with $2n+4$ unknowns $\{q\}$, ω, g, k, V, where n is the number of coordinates (degrees of freedom) in the equation (2).

If the structure of aircraft is non linear then the stiffness matrix $[K]$ depends on $[q]$ or more physically $[K]$ depends on amplitudes of aircraft vibration. Critical flutter conditions are in this case function of the vibration amplitude, which is a new parameter (new unknown) in equations

$$\left(\omega^2\left(\left[M\right]+\rho\left[A(k)\right]\right)-(1+ig)\left[K(q)\right]\right)\{q\}=0, \tag{11}$$

$$\left\{q^H\right\}\{q\}-E=0,$$

$$\mathrm{Im}\left(q_n\right)=0,$$

$$V-\frac{\omega\cdot b}{k}=0,$$

where: E – amplitude level proportional to a total mechanical energy in harmonic vibrations,
$Re\,([K(q)]) = [C(q)]$ – stiffness matrix.

The system of $2n+3$ equations (11) has now $2n+5$ unknowns $\{q\}$, ω, g, k, V and E. It means that the one of parameters (the one of unknowns) must be fixed. For example if $g=0$ during calculations, then continuation solution gives the critical flutter conditions V_F, ω_F, $\{q_F\}$ dependent on vibration amplitude level E (limit cycle solution).

5. HARMONIC BALANCE

Previously described methods are based on the assumption that the aircraft motion is time-harmonic. Consequently, all nonlinearities of the structure must be *harmonically equivalent*. The effective tool in this case is the linearization method based on the principle of *harmonic balance* [5, 6] (*harmonic linearization*), which provides equality of amplitude of linearized system and the amplitude of the fundamental harmonic component of nonlinear system at $\bar{\beta}=\beta\cos\omega t$. For the nonlinear *force-deflection* function the real characteristic $M(\beta)$ (for example: *hinge moment – control surface deflection*) is replaced by the equivalent one

$$M(t)=\mathrm{Re}\left(\beta\left(C+iG\right)e^{i\omega t}\right), \tag{12}$$

defined for the time-harmonic motion $\bar{\beta}=\beta e^{i\omega t}$. Real control surface deflections are:

$$\beta_r=\mathrm{Re}(\bar{\beta})=\beta\cos\omega t. \tag{13}$$

Equivalent stiffness and damping coefficients, C and G, respectively are obtained by balancing the fundamental harmonic term of the Fourier series expansion of $M(\beta_r)$ during a single oscillation period.

Harmonically equivalent stiffness:

$$C(\beta) = \frac{1}{\pi\beta} \int_0^{2\pi} M(\beta \cos\omega t) \cdot \cos\omega t \cdot d(\omega t) \tag{14}$$

and damping

$$G(\beta) = \frac{1}{\pi\beta} \int_0^{2\pi} M(\beta \cos\omega t) \cdot \sin\omega t \cdot d(\omega t) \tag{15}$$

are functions of the amplitude β in harmonic oscillation. Equivalent characteristic (*describing function*)

$$M(\beta_r) = \beta(C\cos\omega t - G\sin\omega t) \tag{16}$$

gives, after transformation, the following equation:

$$M(\beta_r) = M^C(\beta_r) + M^G(\beta_r), \tag{17}$$

where: $M^C(\beta_r) = C(\beta)\beta_r$ – linear function of β_r,

$M^G(\beta_r) = -G(\beta)\sqrt{\beta^2 - \beta_r^2}$ – hysteresis function of β_r.

The nonlinear force-deflection function is replaced after linearization by an equivalent one with elliptical hysteresis. Energy dissipated in one period of oscillation is kept unchanged for the equivalent characteristics

$$E_d = \oint M(\beta_r) \cdot d\beta_r = \pi G \beta^2. \tag{18}$$

The conditions necessary for the application of *harmonic balance* are discussed in detail by Popow & Platow [5] and Shen [6]. The integrals (14, 15) can by calculated analytically only for simple $M(\beta_r)$ functions. Typical examples of analytical describing functions are presented in [6, 7]. For the force-deflection characteristics obtained from tests, the only way to calculate integrals (14, 15) is to use numerical method. Practical tests conducted on aircraft, generally allow for estimation of nonlinearities such as: back-lash, solid friction, spring correctors and deflection stops. If nonlinearities are also found to be dependent upon velocity of the control deflection then the tests are more complex and therefore rarely performed on prototypes of aircraft.

6. THE SET-UP DESCRIPTION

6.1. The model suspension system

The Low Turbulence Wind Tunnel at Institute of Aviation has been chosen to prove the functionality of the new LCO model with computer control of a spring system [24]. This tunnel has a close rectangular test section with size 0.5 x 0.65 m. Maximum flow velocity is 85 m/s and can be controlled in whole range with great accuracy (dynamic pressure accuracy up to 0.1 mm H_2O). It has high stability of flow velocity, which is necessary in the LCO measurements, when even minor changes in velocity can cause changes in amplitudes of flutter modes and transient effects. It is particularly important in the most interesting cases for velocities close to the critical flutter speed or in range of LCO modes. The dimensions and kinematical scheme, of flutter model have been set to perform the tests in the most suitable conditions for validation.

The NACA0012 profile has been chosen for the uniform wing cross section. It is probably the most frequently used profile for basic investigation of non-stationary aerodynamics. The aerodynamic surface span of the wing is 0.5 m and the chord 0.2 m. It is assumed that measurement range of velocity is from 15 m/s to 40 m/s and flutter speed for linear portion of stiffness is about 20 m/s and the frequency range from 5 to 10 Hz, what results in the non-dimensional frequency factor k from 0.15 to 0.3.

The two degrees of freedom flutter model (Fig. 1, 2, 3, 4) was designed to obtain possible low mass and was built of carbon composite excluding joints. The principal goals of the experiments were to prove the effectiveness of the new system of tuning the nonlinear stiffness characteristics of plunge K_h and pitch degrees of freedom K_α .

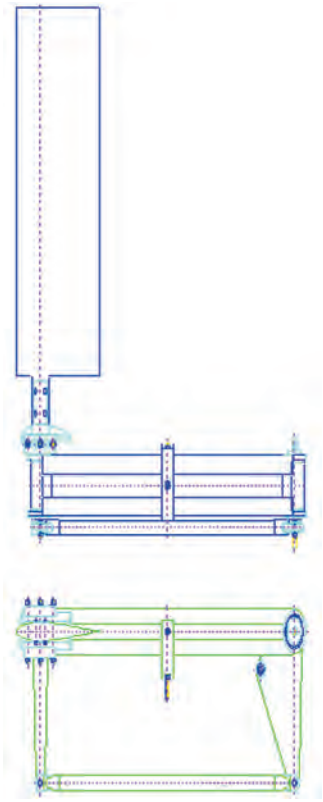

Fig. 1. The design schema

Fig. 2. The view of the LCO model test section

Great flexibility of possible characteristics both with hardening and softening non-linear rule has been obtained by application of the electro-dynamic exciters as the stiffness generators. The exciters were activated by the computer controlled system which produces the programmed displacement-force relation in real time.

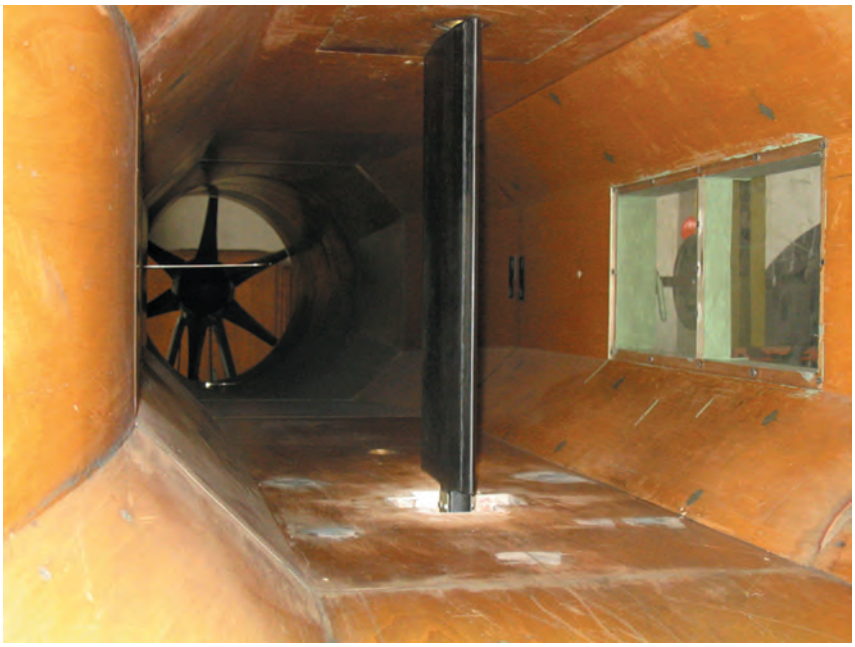

Fig. 3. The overall view of the wind tunnel

Fig. 4. The model suspension system

Using this concept any functional dependence between translation (or rotation) and the exciter force can be easily generated. Also the negative damping forces can be hypothetically produced. The only limitation is the stability of the control circuit where small damping is maintained by means of adjusting the resistor in the exciter coil circuit. The results of the resonance testing (see Table 1) show that the modes of interest i.e. plunge (translation) and pitch (rotation) are well separated from the other vibration modes. No interaction with higher frequency modes should be expected.

Table 1. The results of Ground Vibration Test of the set up

No of event	Mode name	*f* [Hz]	Damping coefficient
mod1031	Plunge (bending)	4.65	0.052
mod1032	Pitch (torsion)	5.71	0.042
mod1004	Vertical bending of arm	30.6	0.011
mod1001	Torsion of arm – low position of the node line	31.9	0.009

Electrodynamics exciters are used as springs (see schema on Fig. 5). Dependence between displacement and force is controlled by the digital computer. In the test set up 12 bits A-D and D-A converters were used. The dependence between displacement and force can be easily digitalized – only 4098 element vector per channel are needed. The control program at the first step calculate matrix of factors, and in the second step in steering loop it doesn't calculate force factor – it simply takes it from the vector.

6.2. Correction of the System Characteristics

The main problem was to obtain proper characteristic of "electronic spring" (Fig. 9). The available electrodynamics exciters are nonlinear. The force factor (dependence of force upon the voltage on entrance of power amplifier) is depending on coil position (Fig. 5, 6). For each of exciter used in tests the measurements of dependence between voltage on power amplifier input and force on the coil were done. The measurements were repeated for several positions of coil. For example results of the measurements for the two positions of coil (5.05 mm and 14.35 mm) are presented on Fig. 7. To adjust the characteristic, the vector of the correction factors has been established and used on each step. The corrected exciter characteristics have been shown on Fig. 8.

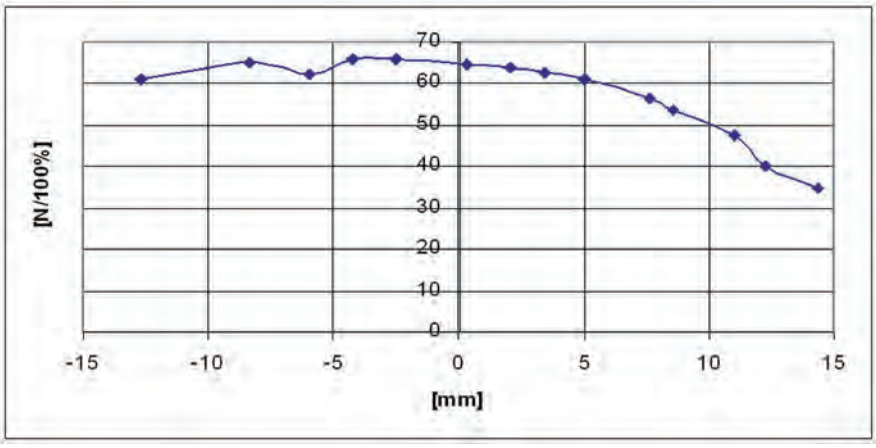

Fig. 5. The force factor – coil deflection relation of the EX 303 exciter

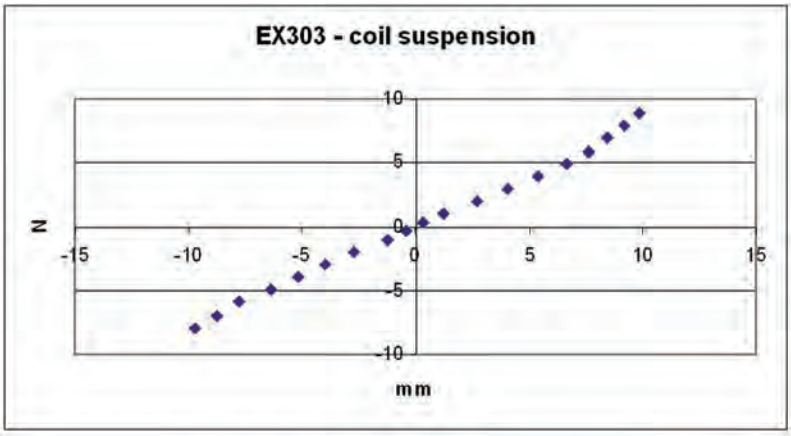

Fig. 6. The force-displacement characteristic of the EX 303 exciter (control off)

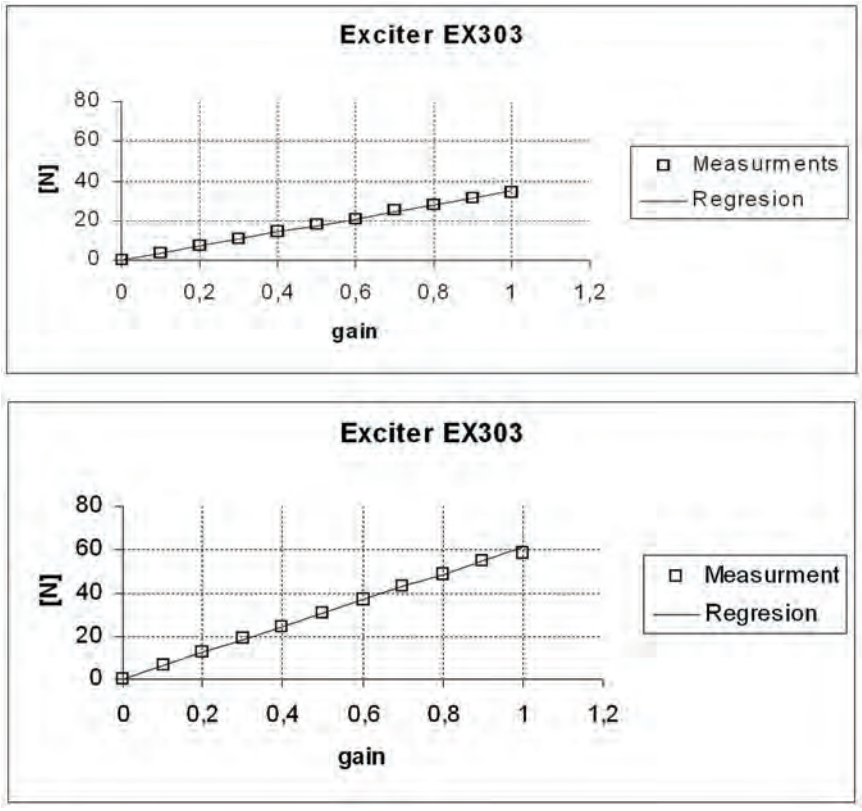

Fig. 7. The dependence between amplifier gain (1 = 100%) and exciter force for selected coil positions: 5.05 mm (up) and 14.35 mm (down)

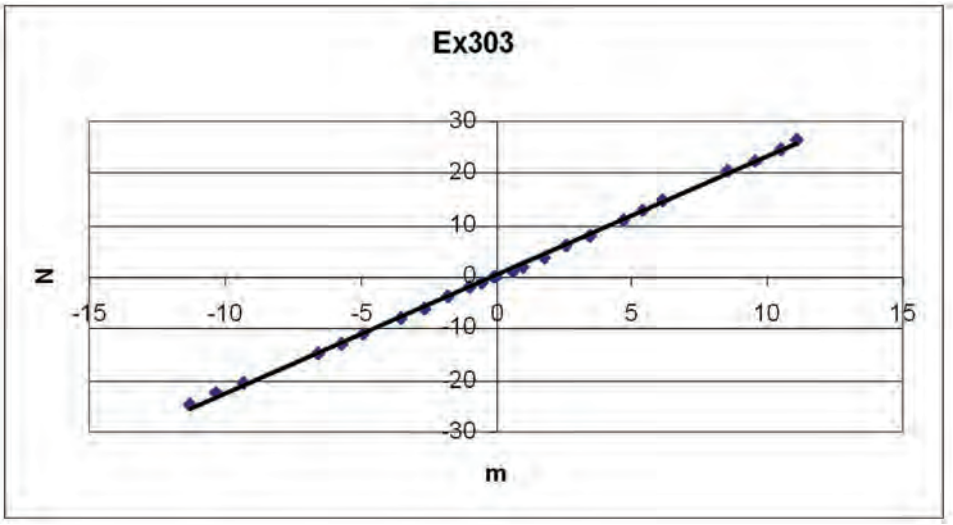

Fig. 8. The dependence between force and displacement of coil (with the digital correction)

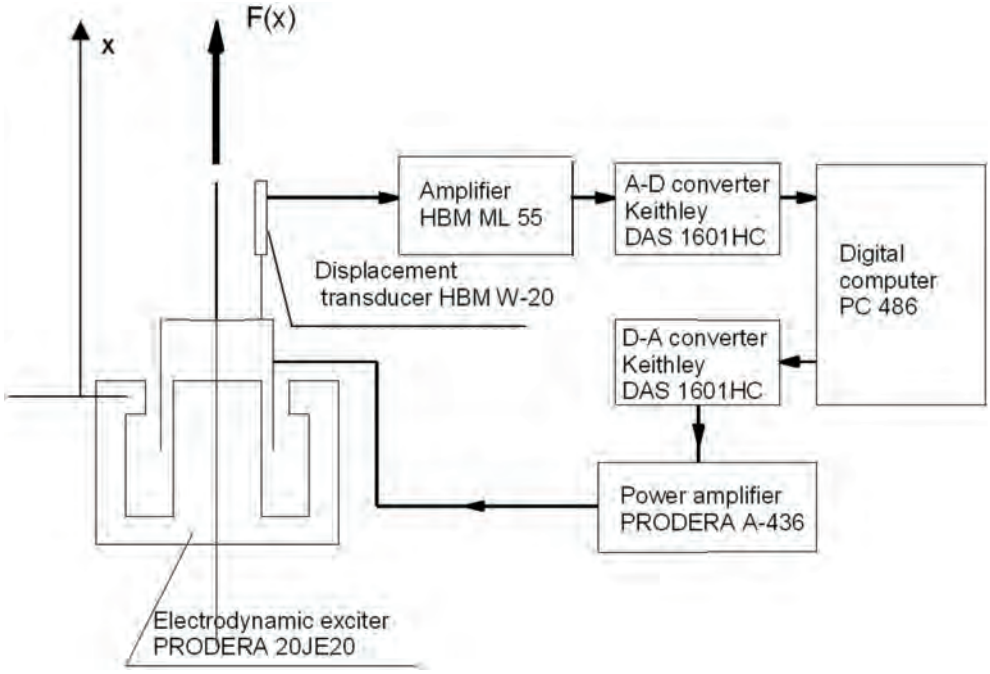

Fig. 9. The block diagram of the „electronic spring" (one channel)

6.3. Tuning nonlinearities

The experimentally measured sets up parameters (reduced to unit span of the wing) are as follow:

$$K_{h0} = 2170 \text{ [N/m]}, \qquad \beta_h = 20000 \text{ [1/m}^2\text{]},$$

$$K_{\alpha 0} = 24.10 \text{ [Nm/rd]}, \qquad \beta_\alpha = 800 \text{ [1/rd}^2\text{]}.$$

Most of wind tunnel tests were performed for cubic nonlinearities:

$$K_h = K_{h0}\,(1 + \beta_h\, h^2), \tag{19}$$

$$K_\alpha = K_{\alpha 0}\,(1 + \beta_\alpha\, \alpha^2) \tag{20}$$

and characteristics of "electronic springs" with this type of nonlinearity are shown on Fig. 10.

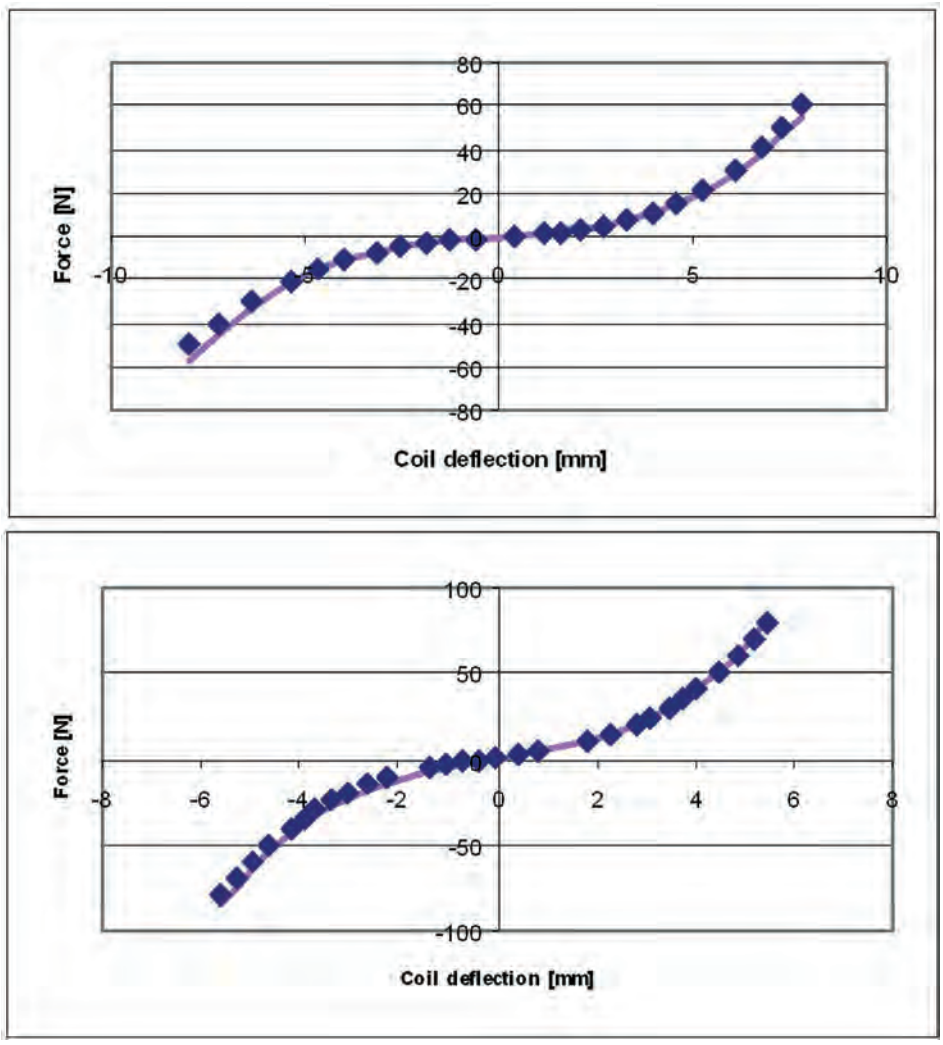

Fig. 10. The comparison between required (fine line) and measured (dots) characteristic of nonlinear spring. Degrees of freedom – plunge (up) and pitch (down)

7. LCO CALCULATIONS COMPARED WITH WIND TUNNEL EXPERIMENT

Harmonic balance and a continuation method were applied to the flutter calculations of two degrees of freedom wing [25], suspended in the wind tunnel by non-linear (cubic) springs (Fig. 1, 2, 3, 4) in plunge and pitch. The PITCON package of FORTRAN subroutines [11] was used to solve the system of equations (11). PITCON was designed at University of Pittsburgh to be a general-purpose package for the solution of undetermined system of non linear equations in which the number of equations is one less than the number of unknowns. Calculation model of the wing is shown on Fig. 11.

The following parameters have been derived from the measurements during the tests:

- dependence of the amplitude of LCO on the velocity,
- phase shift between the modes of vibration plunge (h) and pitch (α).

For each flow velocity, vibrations of model were excited by the step of plunge or pitch. The time histories were recorded. From this data the frequency and the amplitude of the vibration mode have been extracted.

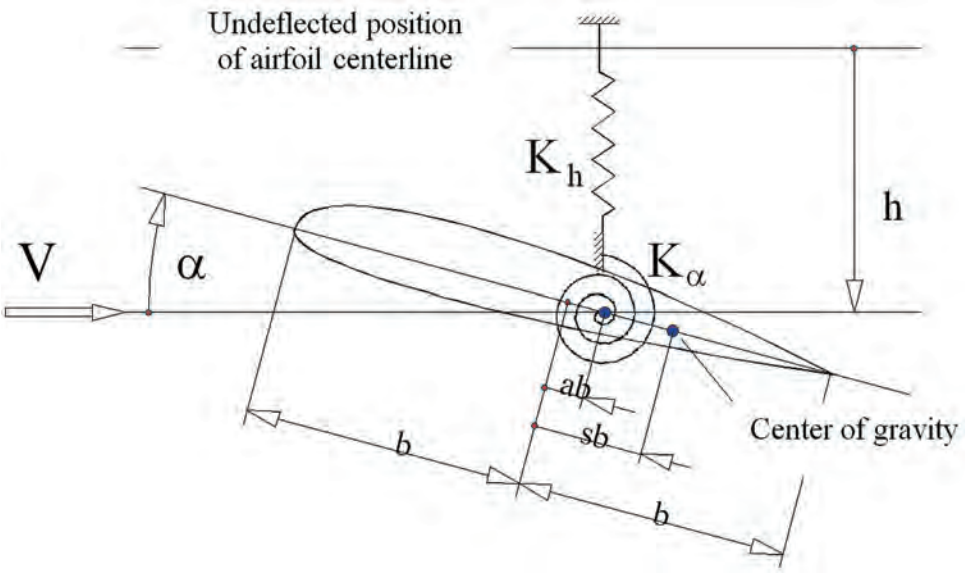

Fig. 11. Two-dimensional wing (airfoil) suspended by plunge and pitch springs

Among others the influence of following parameters on LCO was tested during wind tunnel experiment:

- rotation axis location for one nonlinearity in plunge (test case 1 and 2 and test case 5 and 5a),
- rotation axis location for nonlinearities in plunge and pitch (test case 7 and test case 16),
- one nonlinearity in pitch (test case 13),
- rotation axis location for linear model (test case 6 and test case 14).

The stiffness data of the wing tested in the wind tunnel are listed in the Table 2.

Table 2

Experiment	***a***	K_{h0} **[N/m]**	β_h **[1/m²]**	$K_{\alpha 0}$ **[Nm/rd]**	$\beta\alpha$ **[1/rd²]**	g_h, g_α
Test case 1 and 2	-0.5	2170	20000	24.10	0	(0.025, 0.050, 0.100)
Test case 5 and 5a	-0.6	2170	20000	24.10	0	(0.025, 0.050, 0.100)
Test case 7	-0.6	2170	20000	24.10	800	(0.025, 0.050, 0.100)
Test case 16	-0.7	2170	20000	24.10	800	(0.025, 0.050, 0.100)
Test case 13	-0.6	2170	0	24.10	400	(0.025, 0.050, 0.100)
Test case 6	-0.6	2170	0	24.10	0	(0.025, 0.050, 0.100)
Test case 14	-0.7	2170	0	24.10	0	(0.025, 0.050, 0.100)

where: a – location of the rotation axis,
K_{h0} – (linear) plunge stiffness,
$K_{\alpha 0}$ – (linear) pitch stiffness,
β_h, β_α – nonlinearity factors,
g_h, g_α – artificial damping.

The mass data reduced to the wing span are shown in Table 3.

Table 3

a	*M*[kg/m]	*S*[kgm/m]	*I*[kgm²/m]
-0.5	2.665979	0.0276580	0.0187950

where: *a* – location of the rotation axis,
M – mass,
S – mass static moment relative to the wing rotation axis,
I – mass moment of inertia relative to the wing rotation axis.

7.1. Test case 1 and 2 (nonlinearity in plunge; a = -0.5)

Calculation results compared with the wind tunnel tests are shown on Fig. 12, 13. Test results are indicated by ▲ and +. Calculation results are indicated by solid lines.

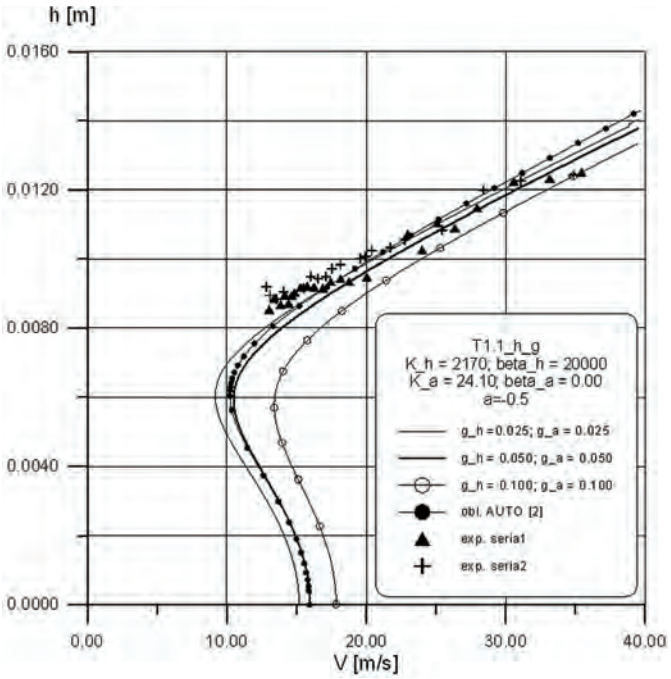

Fig. 12. LCO – plunge

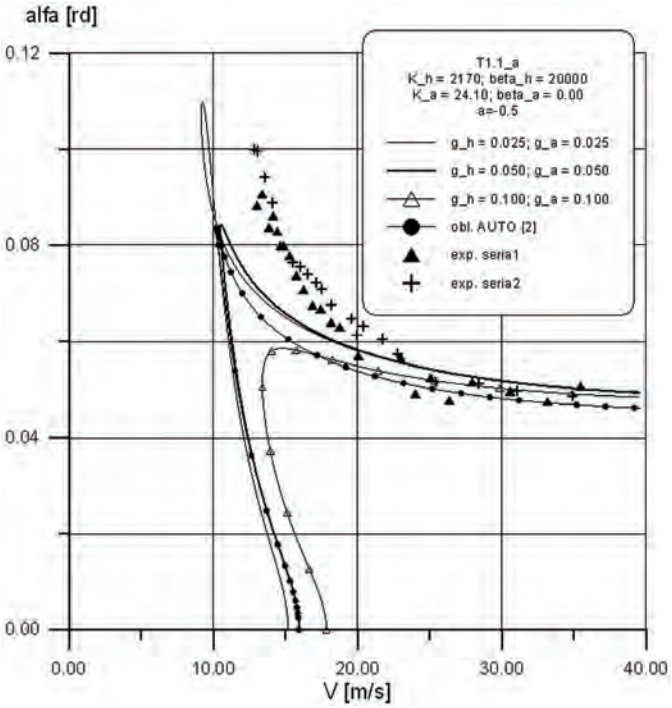

Fig. 13. LCO – pitch

Examples of the time history and the phase shift are shown on Fig. 14 and Fig. 15.

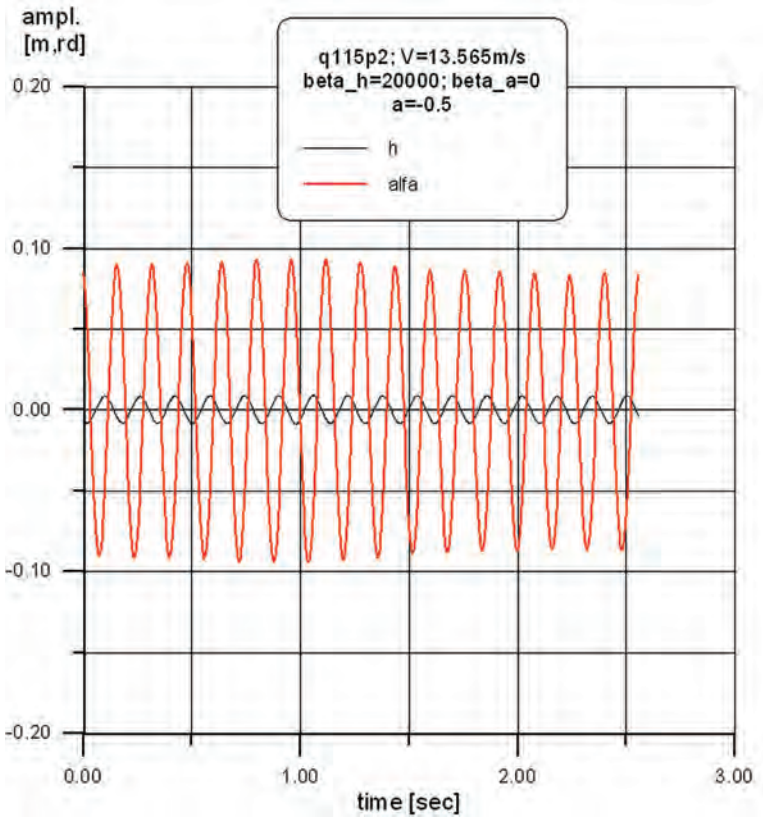

Fig. 14. Plunge and pitch amplitudes (exp.)

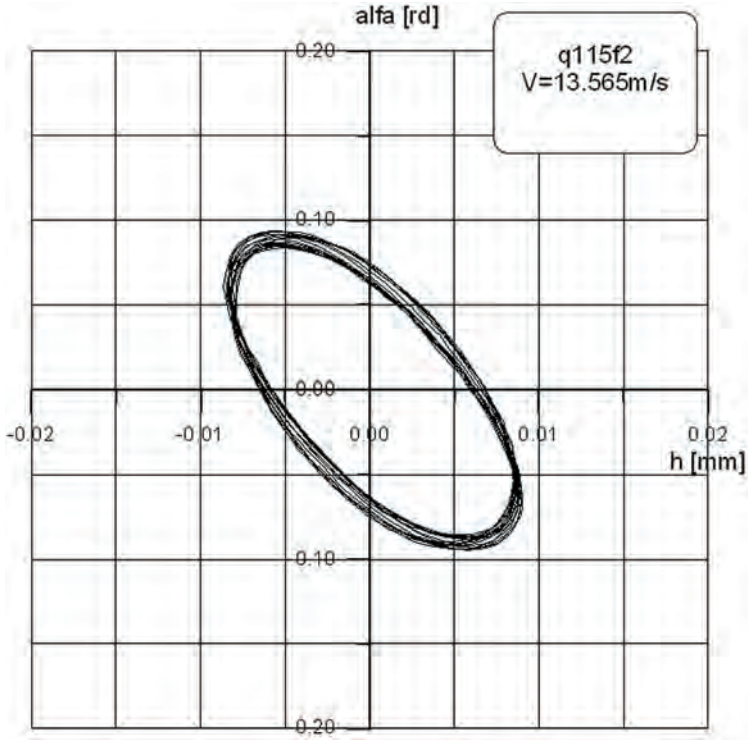

Fig. 15. LCO (wind tunnel experiment)

The graphs were built based on the measured vibration amplitudes during the stable LCO for each wind velocity. In “Test case 1 and 2” vibration were measured for more than 40 velocities. Comparison of LCO obtain by calculations with experiment is very good for plunge and acceptable for pitch.

7.2. Test case 5 and 5a (nonlinearity in plunge; a = -0.6)

Calculation results compared with the wind tunnel tests are shown on Fig. 16, 17. Test results are indicated by ▲ and ■. Calculation results are indicated by solid lines.

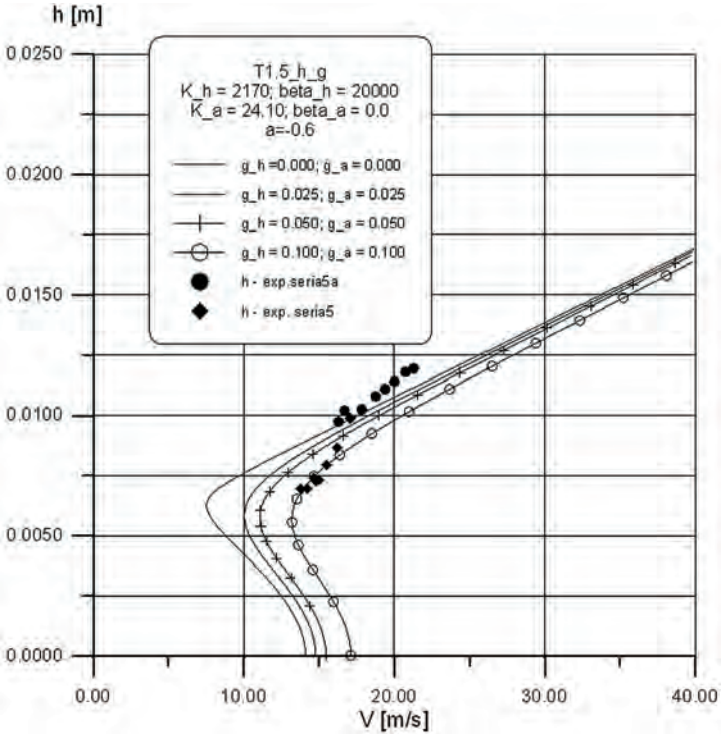

Fig. 16. LCO – plunge

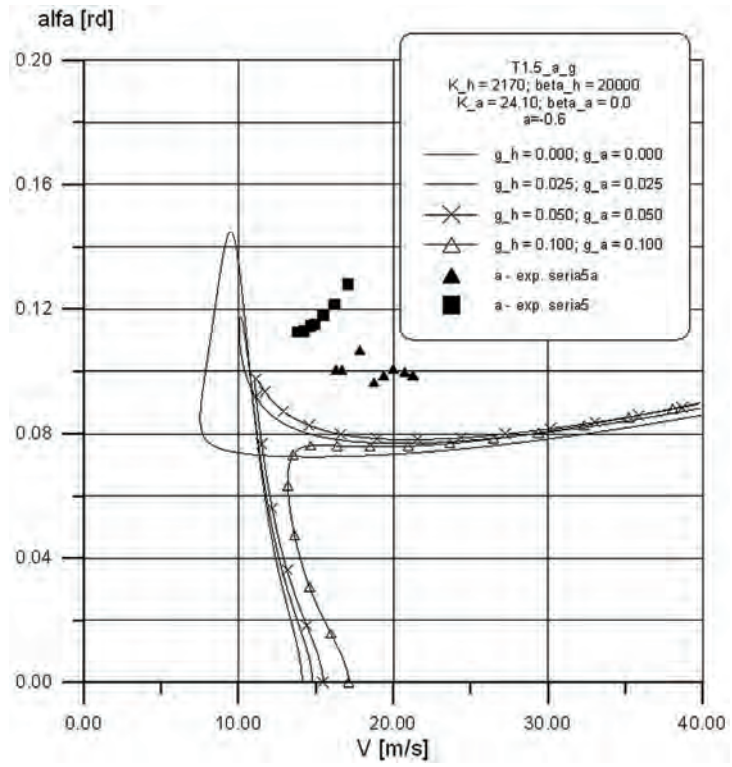

Fig. 17. LCO – pitch

Similar to "Test case 1 and 2" the graphs were build based on the measured vibration amplitudes during the stable LCO for each wind velocity. Two flutter modes with different phase shift between plunge and pitch were obtained in tests.

Examples of the time history and the phase shift in *first mode* are shown on Fig. 18 and Fig. 19.

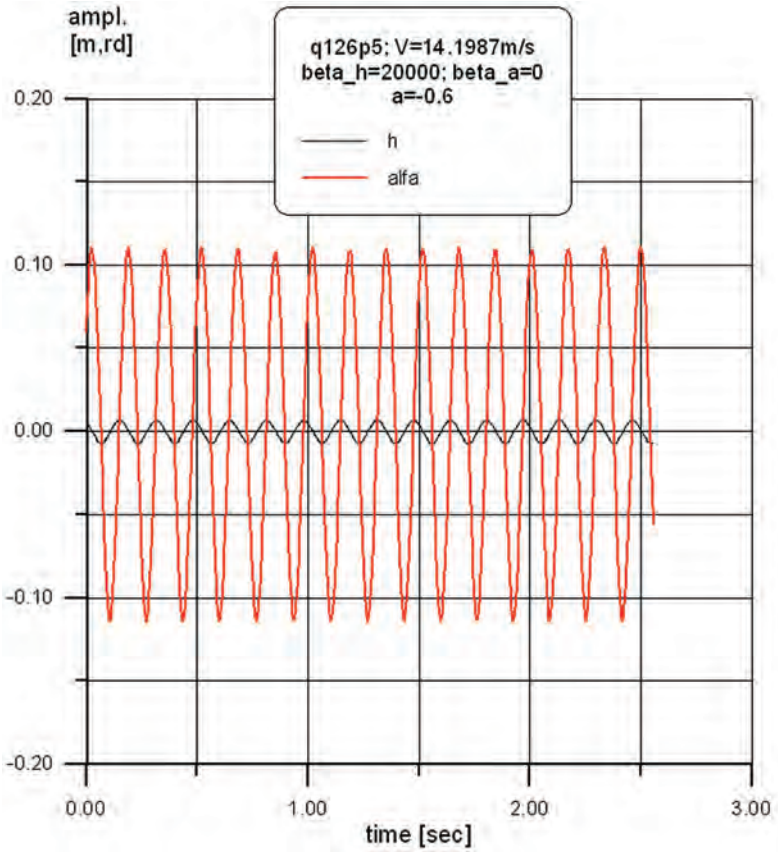

Fig. 18. Plunge and pitch amplitudes (wind tunnel experiment – first mode)

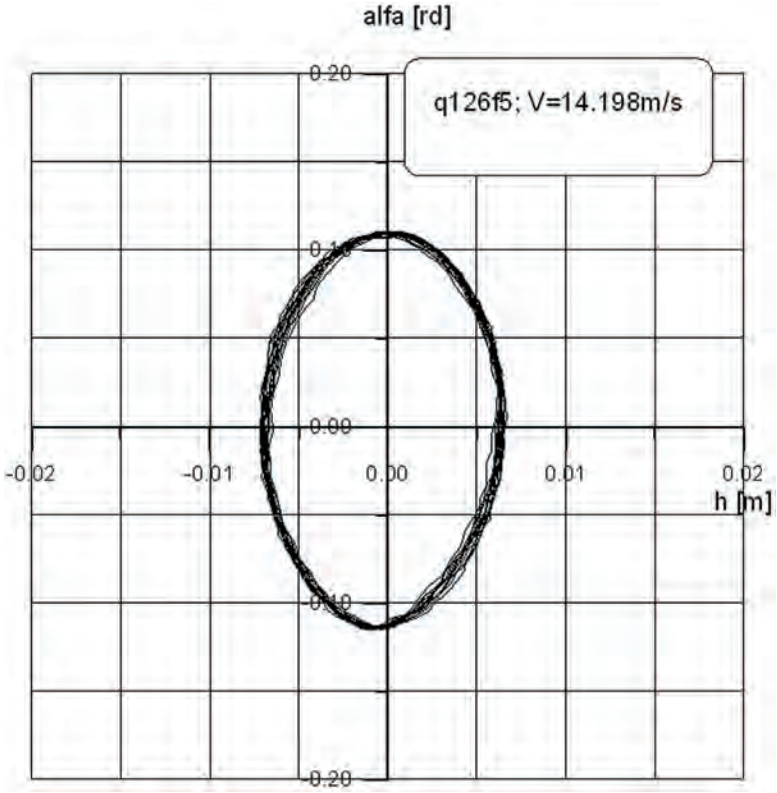

Fig. 19. LCO (wind tunnel experiment– first mode)

Examples of the time history and the phase shift in *second mode* are shown on Fig. 20 and Fig. 21.

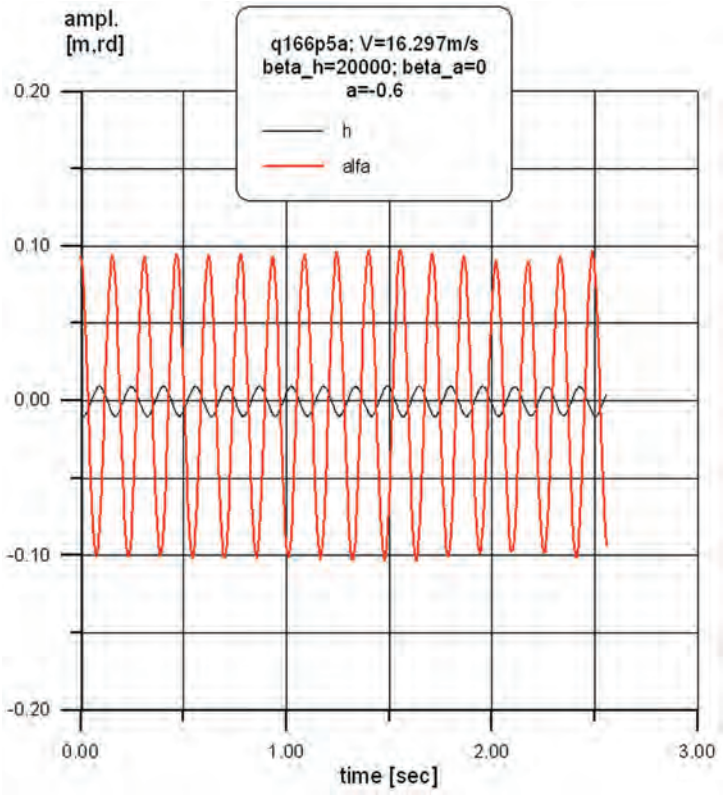

Fig. 20. Plunge and pitch amplitudes (wind tunnel experiment – second mode)

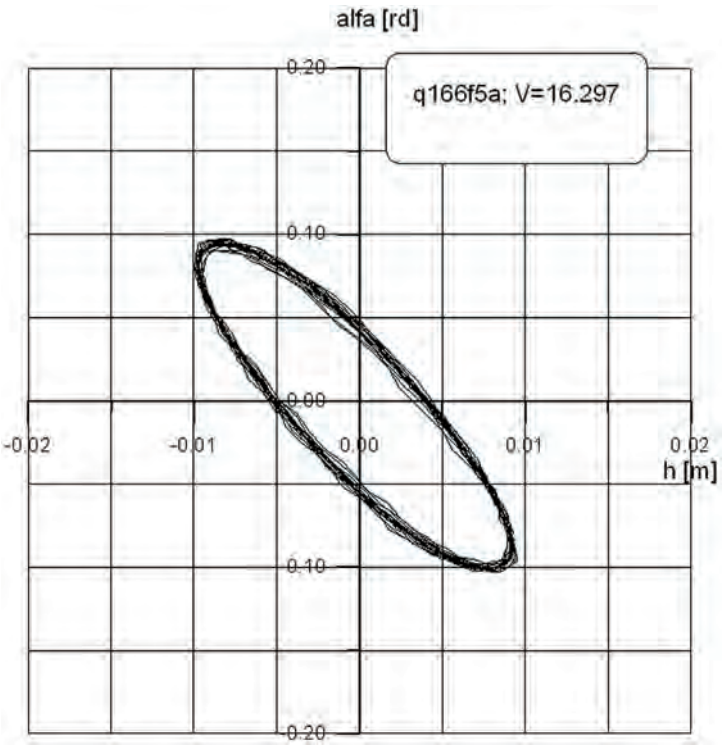

Fig. 21. LCO (wind tunnel experiment – second mode)

In the *first mode* the phase shift between plunge and pitch in LCO is approx. 90° as shown on Fig. 19 while in the *second mode* is more than 270° as shown on Fig. 21. Comparison of LCO obtain by calculations with experiment is very good for plunge and acceptable for pitch.

7.3. Test case 7 (nonlinearities in plunge and pitch; a = -0.6)

Calculation results compared with the wind tunnel tests are shown on Fig. 22, 23. Test results are indicated by ▲ and •. Calculation results are indicated by solid lines.

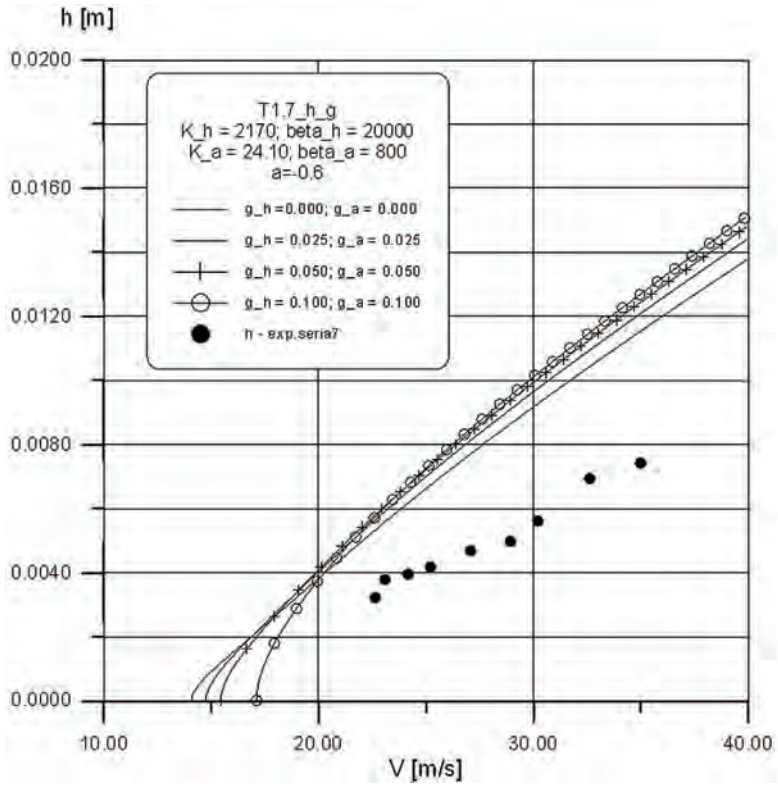

Fig. 22. LCO – plunge

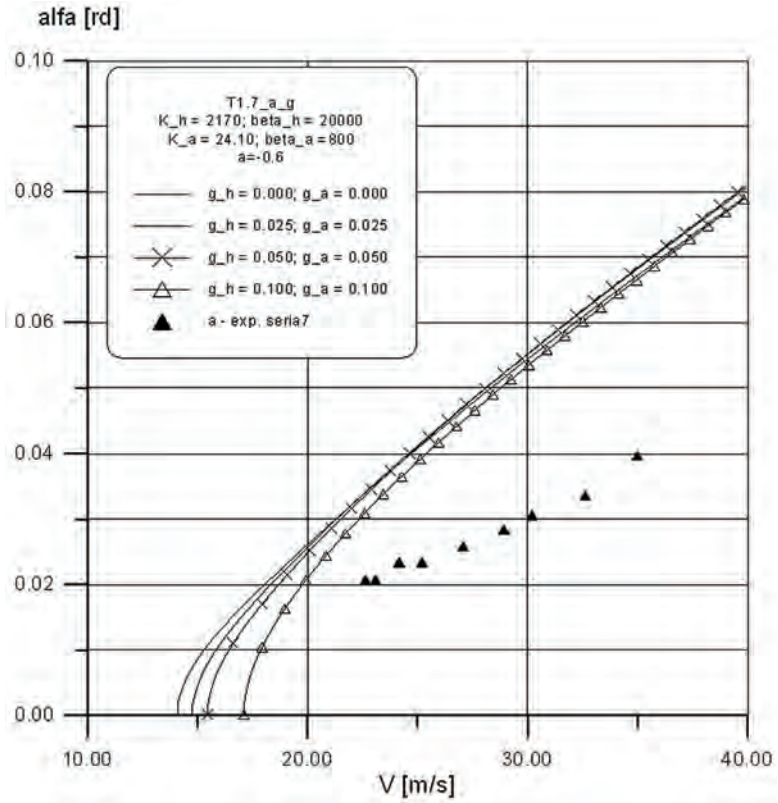

Fig. 23. LCO – pitch

Examples of the time history recorded during wind tunnel tests are shown on Fig. 24, 25 and Fig. 26.

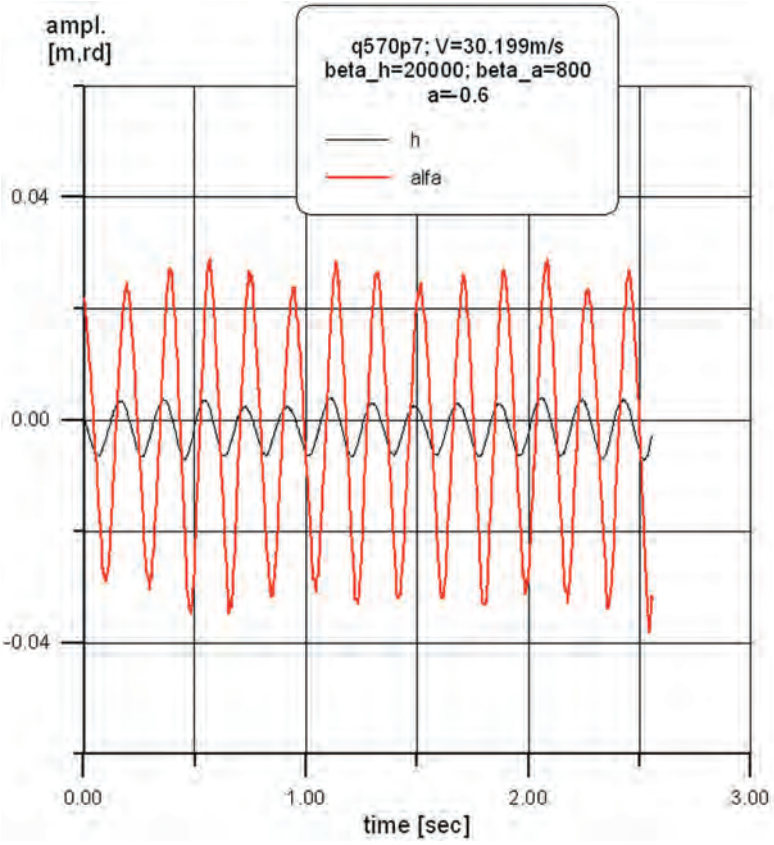

Fig. 24. Plunge and pitch amplitudes (exp.)

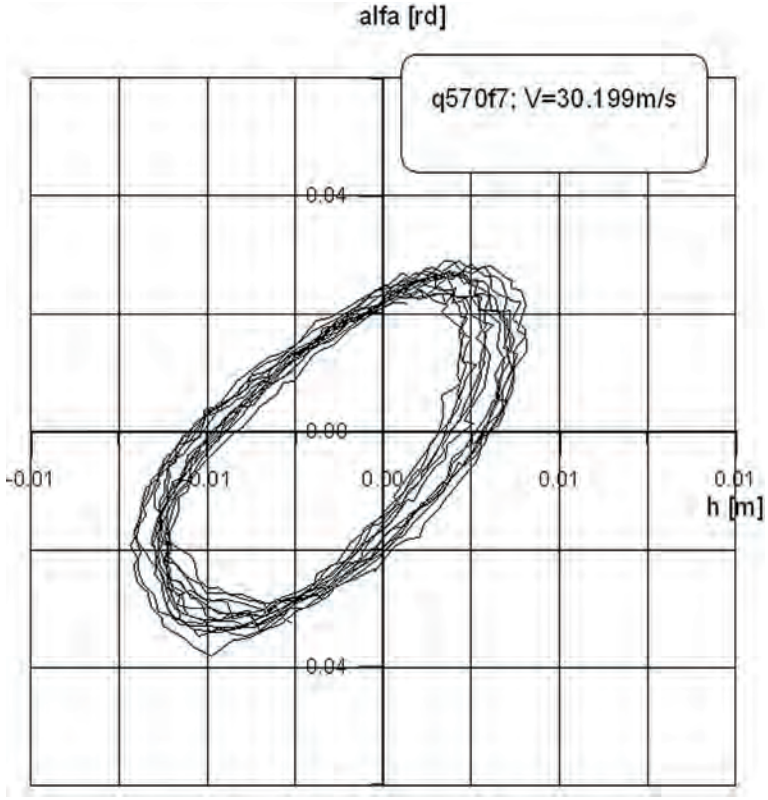

Fig. 25. LCO (wind tunnel experiment)

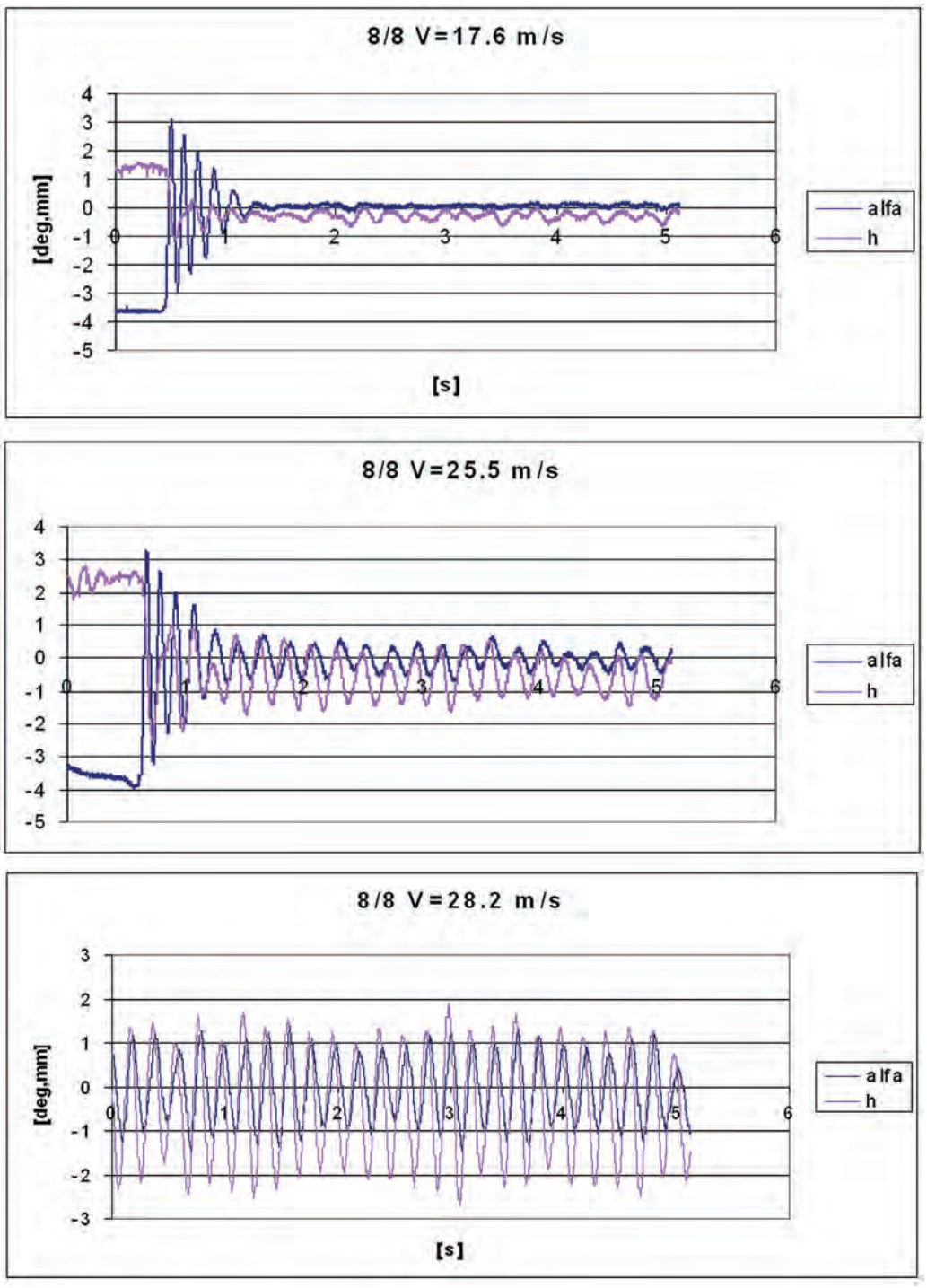

Fig. 26. The measured plunge and pitch for nonlinear LCO [24]

Comparison of LCO obtain by calculations with experiment is qualitative agree for plunge and pitch but amplitudes measured in experiment are approx. 40% lower than calculated ones. Oscillation amplitudes on Fig. 24, 26 show asymmetry relative to the wing mean position during tests and the vibration beat.

7.4. Test case 16 (nonlinearities in plugne and pitch; *a* = -0.7)

Calculation results compared with the wind tunnel tests are shown on Fig. 27, 28.

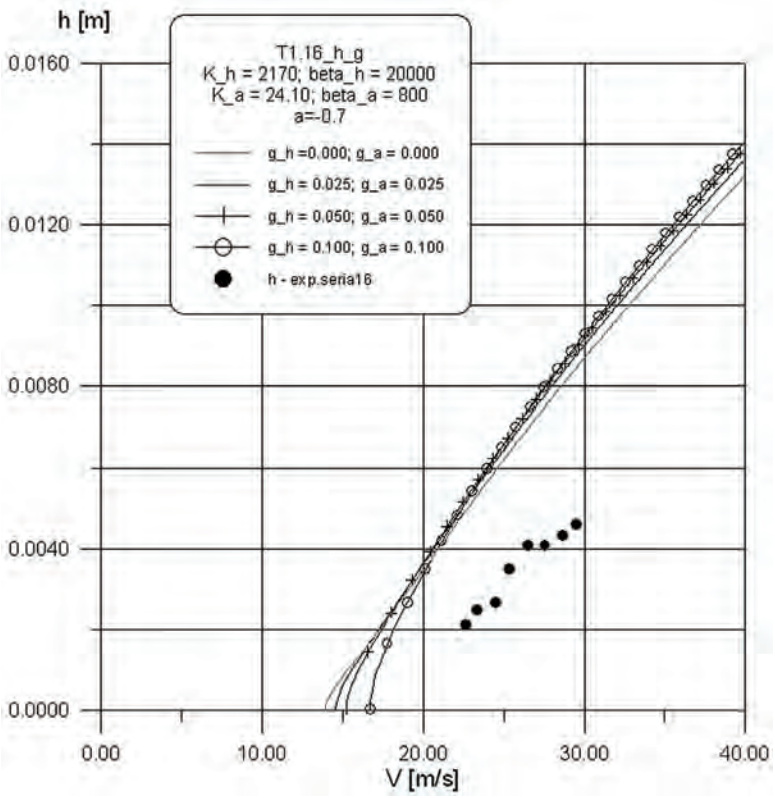

Fig. 27. LCO – plunge

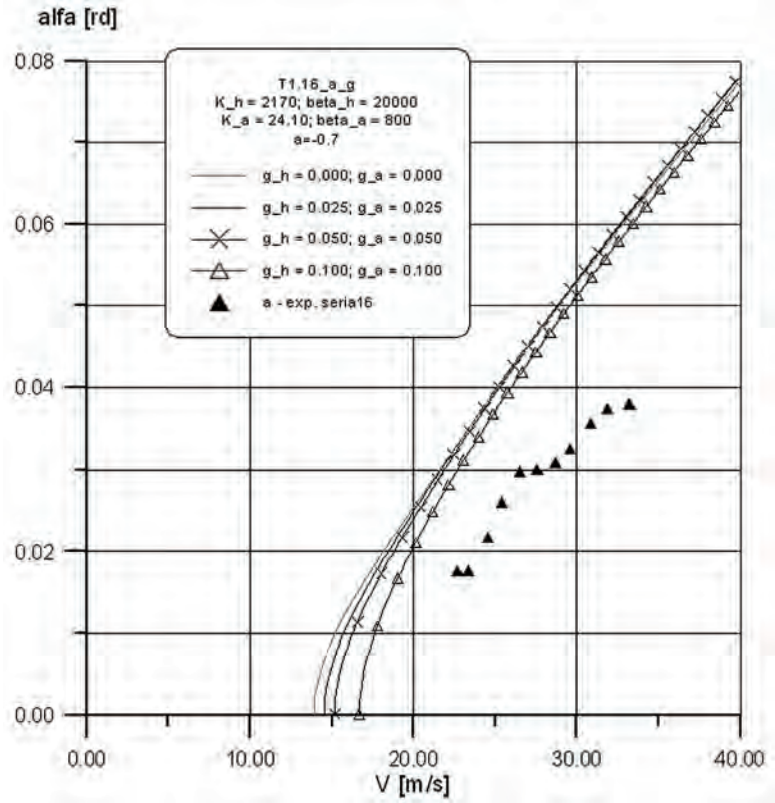

Fig. 28. LCO – pitch

Examples of the time history and the phase shift are shown on Fig. 29 and Fig. 30.

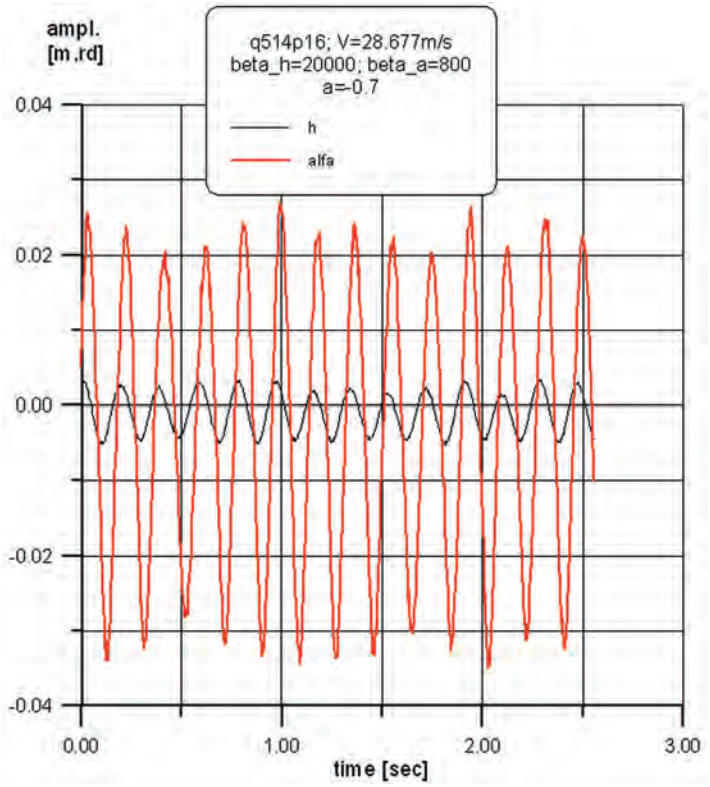

Fig. 29. Plunge and pitch amplitudes (exp.)

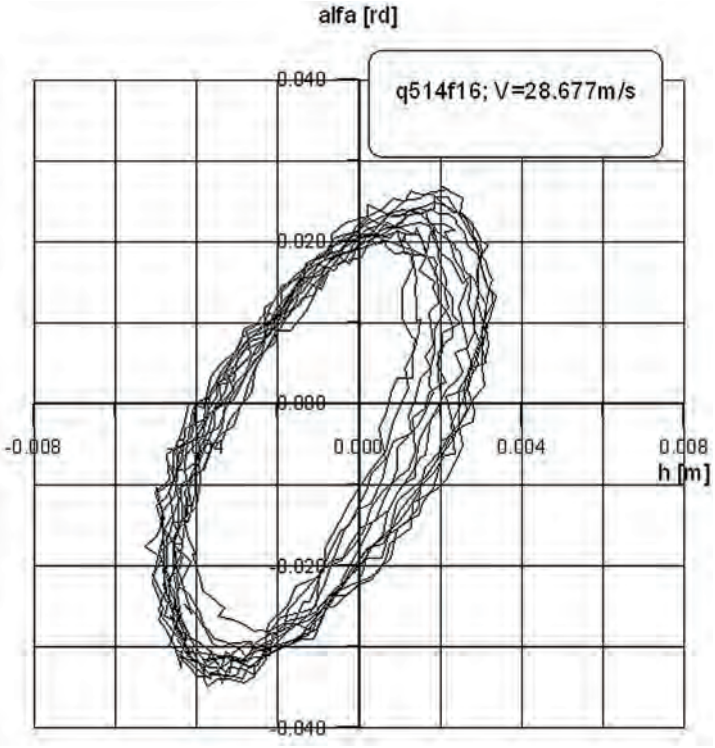

Fig. 30. LCO (wind tunnel experiment)

Comparison of LCO obtain by calculations with experiment is qualitative agree for plunge and pitch but amplitudes of oscillations measured in experiment are approx. 40% lower than calculated ones. Oscillation amplitudes on Fig. 30 show asymmetry relative to the wing mean position during tests and the vibration beat. Vibrations are disturbed by “noise” shown on Fig. 30.

7.5. Test case 13 (nonlinearity in pitch; *a* = -0.6)

Calculation results compared with the wind tunnel tests are shown on Fig. 31, 32.

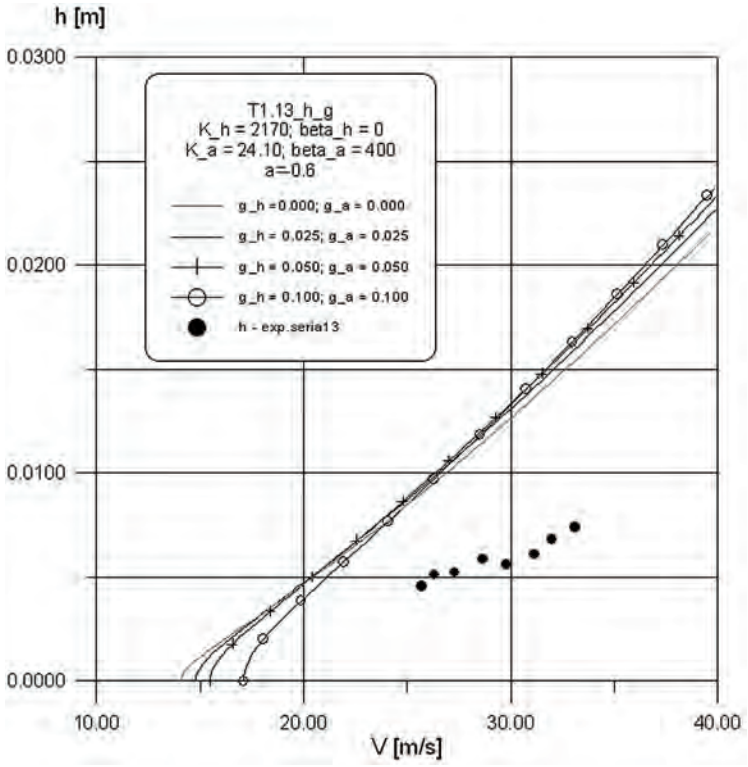

Fig. 31. LCO – plunge

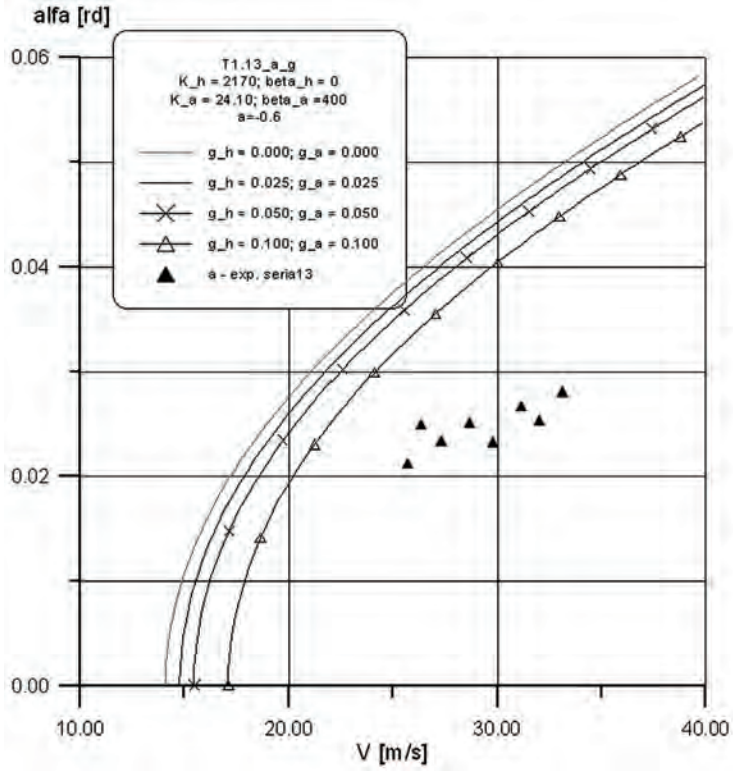

Fig. 32. LCO – pitch

Examples of the time history and the phase shift are shown on Fig. 33 and Fig. 34.

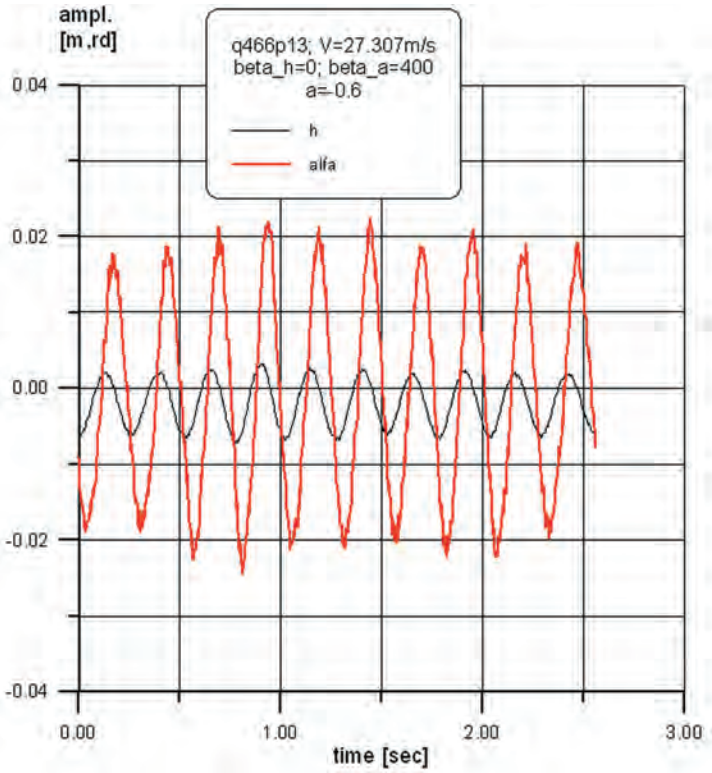

Fig. 33 Plunge and pitch amplitudes (exp.)

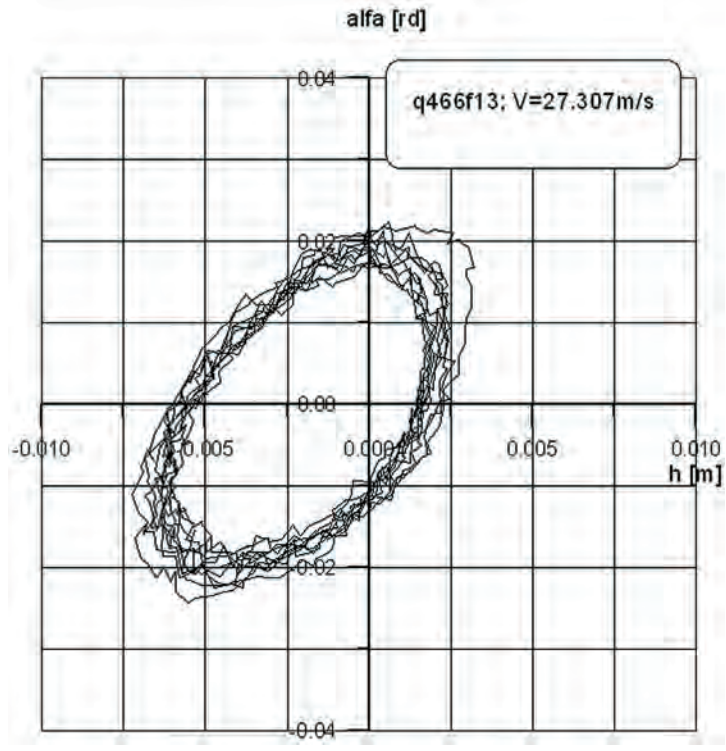

Fig. 34 LCO (wind tunnel experiment)

Comparison of LCO obtain by calculations with experiment is qualitative agree for plunge and pitch but amplitudes of oscillations measured in experiment are approx. 40%÷50% lower than calculated ones. Oscillation amplitudes on Fig. 33 show asymmetry relative to the wing mean position during tests and the vibration beat. Vibrations are disturbed by “noise” shown on Fig. 34.

7.6. Test case 6 (linear model; a = -0.6)

Calculation results compared with the wind tunnel tests are shown on Fig. 35.

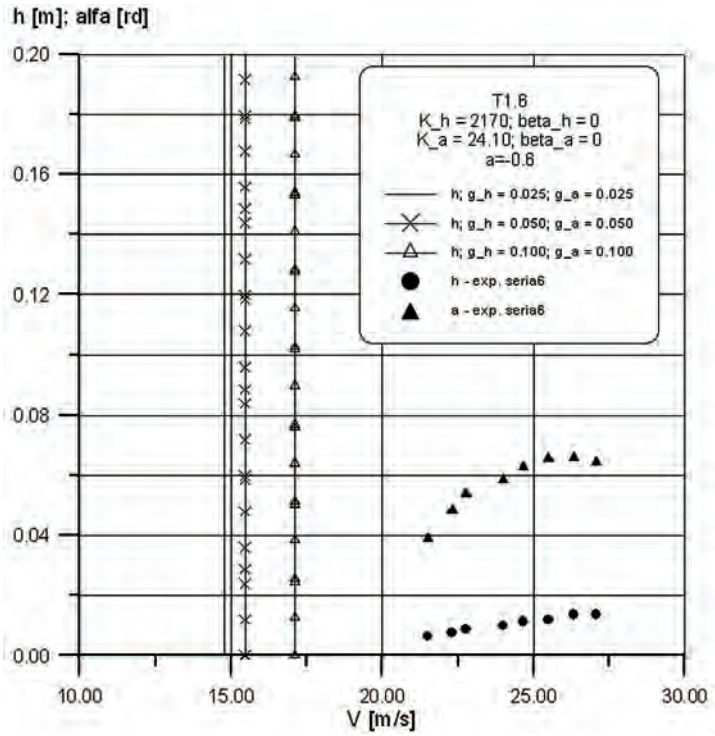

Fig. 35 „Linear" flutter

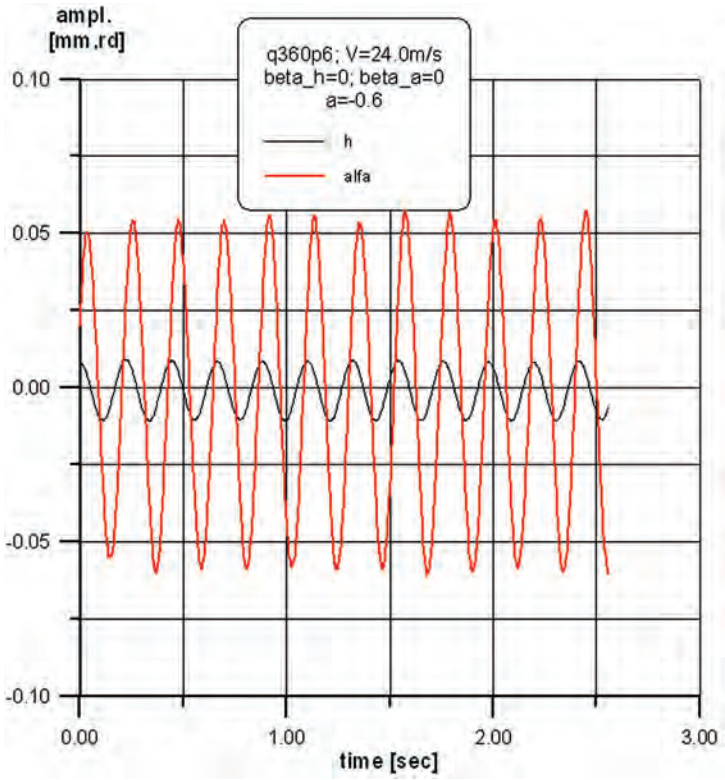

Fig. 36 Plunge and pitch amplitudes (exp.)

Examples of the time history recorded during wind tunnel tests are shown on Fig. 36 and Fig. 37.

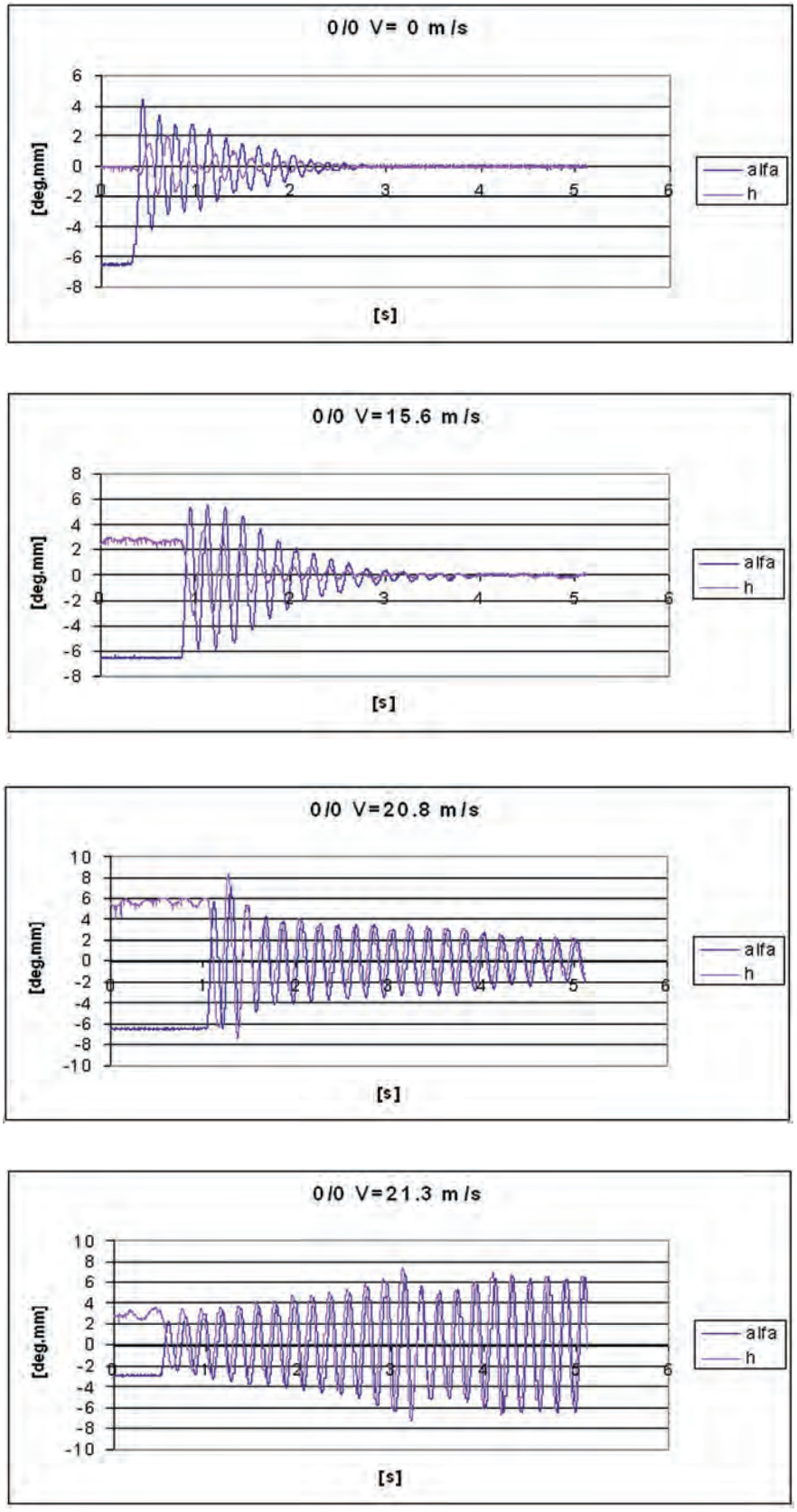

Fig. 37. The measured plunge and pitch for linear case [24]

7.7. Test case 14 (linear model; a = -0.7)

Calculation results compared with the wind tunnel tests are shown on Fig. 38, 39. Test results are indicated by ▲ and ●. Calculation results are indicated by solid lines.

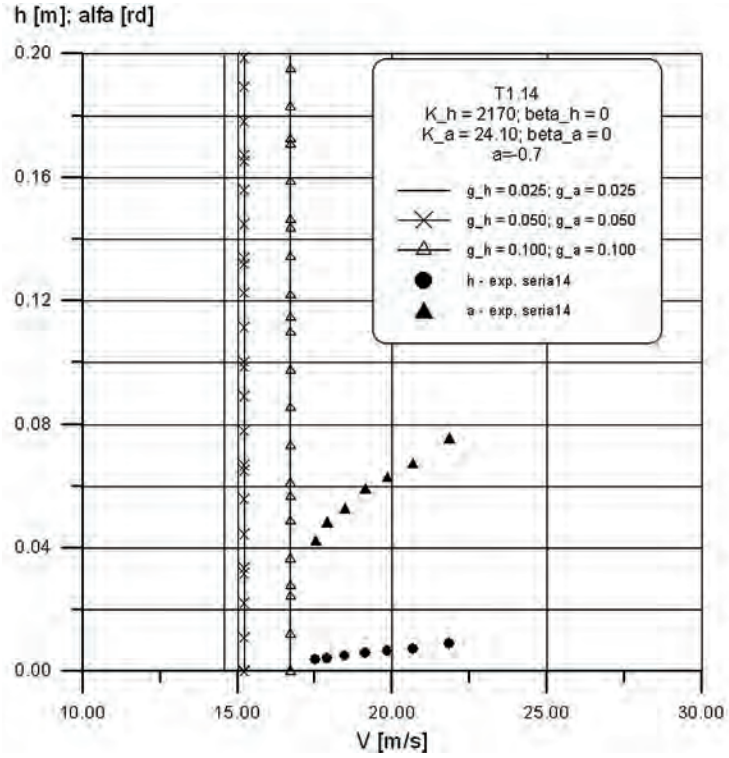

Fig. 38. „Linear" flutter

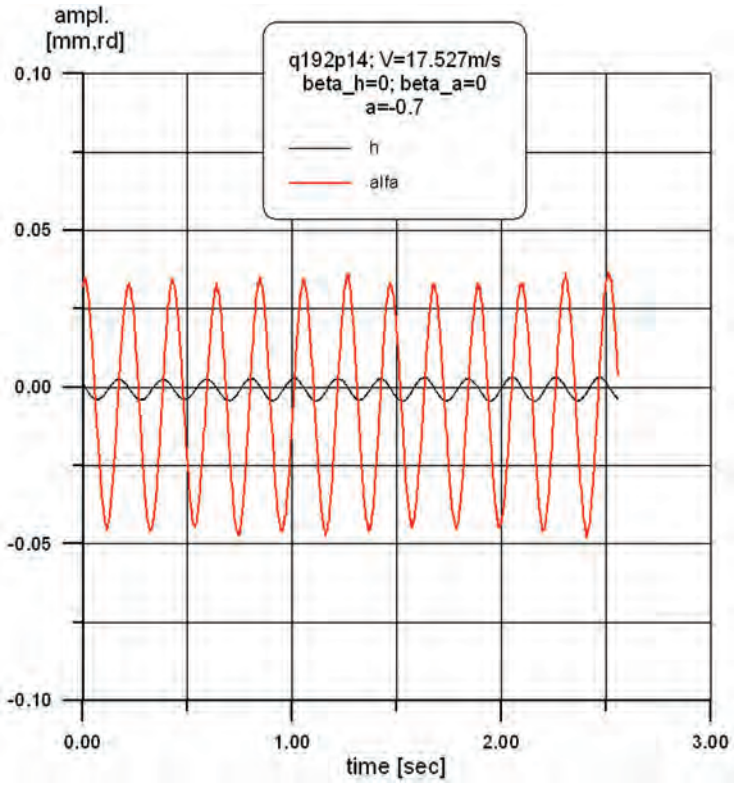

Fig. 39. Plunge and pitch amplitudes (exp.)

In both "linear" wind tunnel tests (case 6 and case 14) LCO was measured. The "linear flutter" was not obtained in experiment. Pitch amplitudes on Fig. 39 show asymmetry relative to the wing mean position during tests.

8. CONCLUSIONS

1. Calculation performed for 2D model based on the harmonic balance and the continuation method show qualitative agreement with wind tunnel experiment.
2. For 2D model with only plunge nonlinear spring, calculations are also quantitatively compatible to wind tunnel experiment.
3. For only pitch nonlinear spring frequency beat and "noise" in main oscillations have been experimentally obtained. Calculation are qualitatively compatible to wind tunnel experiment. Oscillation amplitudes measured in experiment are 20% to 40% lower than calculated.
4. Disagreements between experimental results and calculations as well as non detected "linear flutter" during wind tunnel tests can result from:
   - application of *harmonic-balance*, which is probably to far-going simplification,
   - non identified nonlinearities existing in the test stand.
5. Wind tunnel tests (with controlled nonlinear stiffness) are expensive and difficult to perform.

Acknowledgements

This research was supported by grant No 9T12C06411 from the Polish State Committee for Scientific Research. Some results were presented at NATO AVT-152 Symposium on "Limit-Cycle Oscilations and Other Amplitude-Limited, Self-Excited Vibrations" in Loen, Norway, 2008.

BIBLIOGRAPHY

[1] **Breitbach E.**: *Treatment of the Control Mechanisms of Light Airplanes in the Flutter Clearance Process*, NASA Conference Publication 2085, 1979.

[2] **Breitbach E.**: *Flutter Analysis of an Airplane with Multiple Structural Nonlinearities in the Control System*, NASA TP 1620, March 1980.

[3] **Nowak M., Potkański W.**: *Flutter Analysis of Light Airplanes*, Prace Instytutu Lotnictwa 65, 1976, pp. 3-38.

[4] **Lee C. L.**: *An Iterative Procedure for Nonlinear Flutter Analysis*, AIAA Journal, Vol. 24, May 1986, pp. 833-840.

[5] **Popow E. P., Platow I. P.**: *Approximate Methods in Analysis of Automatic Systems*, Moscow 1960.

[6] **Shen S. F.**: *An Approximate Analysis of Nonlinear Flutter Problems*, Journal of the Aero/Space Sciences, Vol. 28, Jan. 1959, pp. 25-32, 45.

[7] **Breitbach E.**: *Effects of Structural Nonlinearities on Aircraft Vibration and Flutter*, AGARD-R-665, Jan. 1978.

[8] **Lee B. H. K., Leblanc P.**: *Flutter Analysis of a Two-dimensional Airfoil with Cubic Non-linear Restoring Force,* NRC No. 25438, 1986.

[9] **Lee B. H. K., Desrochers J.**: *Flutter Analysis of a Two-dimensional Airfoil Containing Structural Nonlinearities*, NRC No. 27833, 1987.

[10] **Potkański W.**: *Flutter Calculations for a System with Interacting Nonlinearities*, AIAA CP9213, 1992.

[11] **Rheinboldt W. C.**: *Numerical Analysis of Parametrized Nonlinear Equations*, John Wiley&Sons, Inc. 1986.
[12] **Meyer E. E.**: *Application of a New Continuation Method to Flutter Equation*, 29th Structures, Structural Dynamics and Materials Conference, A Collection of Technical Papers, Virginia April 18-20, 1988.
[13] **Potkański W.**: *Practical Investigations of Nonlinearities in Aeroelastic Equations*, Goettingen 1993, (none published).
[14] **Nowak M.**: *Unpublished Communication* (1995).
[15] **Szeląg D.**: *Investigations of an influence of structural nonlinearities on flutter limit cycle*, Final Report (in polish), KBN, 1999.
[16] **Grzedziński J.**: *Flutter Analysis of a Two-Dimensional airfoil with nonlinear springs based on center-manifold reduction*, Arch.Mech., 46, (1994), pp. 735-755.
[17] **Yang Y. R., Zhao L. C.**: *Subharmonic bifurcation analysis of wing with store flutter*, J. of Sound and Vibration, 157, (1992), pp. 477-484.
[18] **Potkański W.**: *Flutter analysis for a system with Interacting Nonlinearities*, International Forum on Aeroelasticity and Structural Dynamics 1991, Aachen, DGLR-Bericht no 91-06, pp. 315-318.
[19] **McIntosh S. C. Jr., Reed .E. Jr., Roden W.P.**: *Experimental and theoretical study of nonlinear flutter*, J. Aircraft, 18, (1981), pp. 1057-1063.
[20] **Yang Y. R., Zhao L. C.**: *Analysis of limit cycle flutter of an airfoil in incompressible flow*, J. of Sound and Vibration, 123, (1988), pp. 1-13.
[21] **Zeng Y., Singh N.**: *Output feedback variable structure adaptive control of an aeroelastc system*, J. of Guidance and Control, Vol. 21 (1999), No 6, pp 830-837.
[22] **Kiessling F., Potkański W.**: *Non-Linear Flutter Analysis by a Continuation Method*, 2nd International Conference Engineering Aero-Hydroelasticity, Pilsen – Czech Republic, June 6-10, 1994, pp. 221-226.
[23] **Potkański W.**: *Nonlinear flutter analysis by application of a harmonic balance and a continuation method. Proc. of the second seminar on recent research and design progress in aeronautical engineering and its influence on education (part 2)*. Institute of Aeronautics and Applied Mechanics, Warsaw University of Technology, Research Bulletin, No 7 (1997).
[24] **Szeląg D., Lorenc Z., Fornasier L., Posadzy P.**: *A Digitally Controlled Suspension System for the Real Time Generation of the Structural Nonlinearities in the Flutter Wind Tunnel Validation Testing*, IFASD 2005 – Munich, DGLR-Bericht 2005-4.
[25] **Potkański W.**: *Determination of LCO Parameters by the Harmonic Balance and the Continuation Method – Part II Calculation Results*, Institute of Aviation Internal Report No. 83/BP/98.

W. Potkański, Z. Lorenc, D. Szeląg

OBLICZENIA LCO PORÓWNANE Z BADANIAMI DWUWYMIAROWEGO MODELU FLATTEROWEGO W TUNELU AERODYNAMICZNYM

Streszczenie

Klasyczna analiza flatteru współczesnych samolotów polega na poszukiwaniu najniższej (krytycznej) prędkości flatteru w zadanych warunkach oraz zmiany tej prędkości przy zmianach niektórych parametrów układu (samolotu). Badania statyczne i badania rezonansowe prototypów samolotów wykazują zwykle istnienie nieliniowości strukturalnych co skutkuje oscylacjami o ograniczonej amplitudzie (cykle graniczne – LCO). Linearyzacja harmoniczna i metoda kontynuacyjna, opisana w artykule, była z powodzeniem stosowana wcześniej do wyznaczenia cykli granicznych (LCO) dla profilu o dwóch stopniach swobody z nieliniową sztywnością skrętną oraz dla szybowca z nieliniowymi układami sterowania klap, lotek i steru wysokości. Do badań doświadczalnych LCO wykorzystano „sztywny model flatterowy skrzydła" zawieszony w tunelu aerodynamicznym w sposób umożliwiający niezależne przemieszczenia translacyjne i obrotowe oraz symulację nieliniowych sztywności przy tych przemieszczeniach. Nieliniowości generowane były w eksperymencie przy pomocy układu elektro-mechanicznego co pozwoliło na efektywne badanie wpływu różnych charakterystyk sprawnościowych na LCO. Badania były przeprowadzone w Tunelu Niskiej Turbulencji w Instytucie Lotnictwa w Warszawie. W artykule porównano wyniki obliczeń cyklu granicznego z wynikami badań doświadczalnych.

В. Потkански, З. Лоренц, Д. Шелонг

РАСЧЁТЫ LCO И ИХ СРАВНЕНИЕ С РЕЗУЛЬТАТАМИ ИССЛЕДОВАНИЙ ДВУХРАЗМЕРНОЙ ФЛАТТЕРНОЙ МОДЕЛИ В АЭРОДИНАМИЧЕСКОЙ ТРУБЕ

Резюме

Классический анализ флаттера современних самолётов заключается в поисках наименьшей (критической) скорости флаттера в данных условиях и изменения этой скорости при изменениях некоторых параметров системы (самолёта). Статические и резонансовые исследования прототипов самолётов показывают обычно существование структурных нелинейностей, что сказывается осциляциями с ограниченной амплитудой (граничные циклы – LCO). Гармоническая линеаризация и метод континуации описанные в статье были успешно применены раньше для определения граничных циклов (LCO) профиля с двумя степенями свободы и с нелинейной крутильной жёсткостью и дла планера с нелинейными системами управления закрылками, элеронами и рулём высоты. Для экспериментальных исследований LCO была применена „жёсткая, флаттерная модель крыла" подвешенная в аэродинамической трубе таким образом, чтобы перемещения трансляции и оборота были независимыми и чтобы можно было симулировать нелинейную жёсткость при этих перемещениях. Нелинейности задавались во время эксперимента с помощью электромеханической системы, что позволило успешно исследовать влияние разных жёсткостных характеристик на LCO. Исследования проводились в Аэродинамической Трубе Малой Турбуленции в Институте Авиации в Варшаве. В статье сравниваются результаты рассчётов граничного цикла с результатами экспериментальных исследований.